



A thrust network approach to the equilibrium problem of unreinforced masonry vaults via polyhedral stress functions

Fernando Fraternali *

Department of Civil Engineering, University of Salerno, 84084 Fisciano (SA), Italy

ARTICLE INFO

Article history:

Received 13 October 2009

Received in revised form 24 December 2009

Available online 6 January 2010

Keywords:

Thrust network approach

Masonry vaults

No-tension model

Stress function

Crack pattern

Mesh adaption

ABSTRACT

The equilibrium problem of unreinforced masonry vaults is analyzed via a constrained thrust network approach. The masonry structure is modeled as no-tension membrane (thrust surface) carrying a discrete network of compressive singular stresses, through a non-conforming variational approximation of the continuous problem. The geometry of the thrust surface and the associated stress field are determined by means of a predictor–corrector procedure based on polyhedral approximations of the thrust surface and membrane stress potential. The proposed procedure estimates the regions exposed to fracture damage according to the no-tension model of the masonry. Some numerical results on the thrust network and crack pattern of representative vault schemes are given.

© 2010 Elsevier Ltd. All rights reserved.

1. Introduction

The use of force network models for the form finding and stability analysis of masonry vaults and domes has attracted the interest of architects and scientists since antiquity. Some of the main ingredients of such models are the determination of funicular curves (or inverted hanging chains) of given force systems (Poleni, 1991; Heyman, 1966); the slicing technique for the subdivision of 2D thrust surfaces into suitable arches or strips (Wittmann, 1879; Ungewitter, 1890; Heyman, 1966, 1977; Boothby, 2001; Como, 2010); physical or virtual hanging chain models (Tomlow et al., 1989; Kilian and Ochsendorf, 2005; Andreu et al., 2007; Kilian, 2007), famous for their use in the architecture by Antoni Gaudí; and the equilibrium approach to the limit analysis of no-tension structures (Heyman, 1966, 1995; Del Piero, 1998; Huerta, 2001). The latter allows the designer to formulate the structural stability problem as the search for at least one purely compressive state of thrust in equilibrium with the applied loads. Recent contributions to the ongoing research in this area have been proposed by O'Dwyer (1999), Fraternali (2001), Fraternali et al. (2002a,b), Block and Ochsendorf (2005, 2007), and Ochsendorf and Block (2009), dealing with analytical, computational and graphical methods for the design of statically admissible thrust networks. Particularly interesting is the use of polyhedral stress potentials to generate equilibrated force networks (Fraternali et al., 2002a,b). For a review of the available approaches to the statics of masonry vaults and do-

mes we refer the reader to Di Pasquale (1975), Heyman (1995), Lucchesi et al. (2008), Tomasoni (2008), Como (2010), and Block (2009).

This work presents a thrust network approach (TNA) to the equilibrium problem of unreinforced masonry vaults. The proposed TNA assumes that such structures resist to the external loads through a compressive membrane state of stress “condensed” across a material surface S (thrust surface), which is contained in a bounded region of the 3D space. The membrane stress is described through a discrete network of compressive forces, according to the no-tension model of masonry (Giaquinta and Giusti, 1985; Del Piero, 1989; Heyman, 1995). Use is made of a variational formulation of the membrane equilibrium problem, and polyhedral test functions for the thrust surface and membrane stress potential. An iterative procedure is proposed to enforce the no-tension constraint and suitable geometric bounds on the thrust surface, through geometrical and topological adaption of an initial candidate solution. Numerical results are given for a hemispherical dome, a groin vault, and a cloister vault, predicting equilibrated thrust networks and associated crack patterns of the examined structures, and showing the ability of the proposed TNA in predicting frequently observed real crack mechanisms.

2. A variational formulation of the equilibrium of masonry vaults

Let us refer to a masonry vault as a no-tension membrane or thrust surface S contained in a bounded region of the 3D space

* Tel.: +39 089 964083.

E-mail address: f.fraternali@unisa.it.

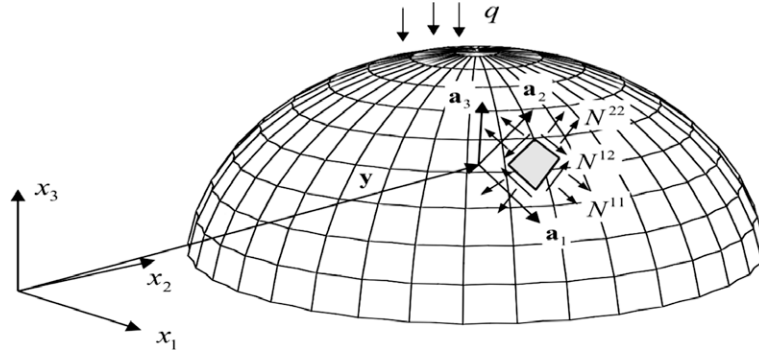


Fig. 1. Thrust surface S.

(Fig. 1). We introduce the projection \$\Omega\$ of \$S\$ onto the horizontal plane (platform of \$S\$), and Cartesian coordinates \$\{x_1, x_2, x_3\}\$, with unit base vectors \$\{\mathbf{e}_1, \mathbf{e}_2, \mathbf{e}_3\}\$, such that \$x_3\$ is perpendicular to \$\Omega\$. Looking at \$x_1\$ and \$x_2\$ as curvilinear coordinates on \$S\$ (Monge's coordinates), we are led to define the following covariant base vectors

$$\mathbf{a}_1 = \mathbf{e}_1 + \partial f / \partial x_1 \mathbf{e}_3, \quad \mathbf{a}_2 = \mathbf{e}_2 + \partial f / \partial x_2 \mathbf{e}_3, \quad \mathbf{a}_3 = 1 / J \mathbf{a}_1 \times \mathbf{a}_2, \quad (1)$$

where \$f = f(x_1, x_2)\$ is a function describing the graph of \$S\$ (shape function of the thrust surface), and it results:

$$J = \sqrt{1 + (\partial f / \partial x_1)^2 + (\partial f / \partial x_2)^2}. \quad (2)$$

It is convenient to project the equilibrium equations of \$S\$ onto the non-orthogonal basis \$\{\mathbf{e}_1, \mathbf{e}_2, \mathbf{a}_3\}\$, obtaining:

$$\frac{\partial P^{\alpha\beta}}{\partial x_\beta} + q_{(\alpha)} = 0, \quad \frac{\partial^2 f}{\partial x_\alpha \partial x_\beta} P^{\alpha\beta} - \frac{\partial f}{\partial x_\alpha} q_{(\alpha)} + q_{(3)} = 0 \quad (\text{summation on } \alpha, \beta). \quad (3)$$

Here, \$q_{(i)}\$ (\$i = 1, 2, 3\$) denote the external forces per unit area of \$\Omega\$ acting on \$S\$, while \$P^{\alpha\beta} = J N^{\alpha\beta}\$ (\$\alpha, \beta = 1, 2\$) denote the projections of the membrane stress resultants \$N^{\alpha\beta}\$ (Fig. 1) onto \$\Omega\$. Assuming pure vertical loading (\$q_{(1)} = q_{(2)} = 0\$), we derive the projected stresses \$P^{\alpha\beta}\$ from the Airy potential (or stress function) \$\varphi\$ such that:

$$P^{11} = \partial^2 \varphi / \partial x_2^2, \quad P^{22} = \partial^2 \varphi / \partial x_1^2, \quad P^{12} = -\partial^2 \varphi / \partial x_1 \partial x_2, \quad (4)$$

reducing (3) to the second order differential equation:

$$a_{\alpha\beta} \partial^2 \varphi / \partial x_\alpha \partial x_\beta - q = 0 \quad \text{in } \Omega, \quad (5)$$

where

$$a_{11} = \partial^2 f / \partial x_2^2, \quad a_{22} = \partial^2 f / \partial x_1^2, \quad a_{12} = -\partial^2 f / \partial x_1 \partial x_2, \quad q = -q_{(3)}.$$

If the surface tractions along the boundary of \$S\$ are prescribed, one can solve (5) with the aid of the boundary condition

$$\varphi = \mu(s) \quad \text{on } \partial\Omega \quad (6)$$

where \$s\$ is the arc-length of \$\partial\Omega\$, and \$\mu(s)\$ is the moment of the boundary tractions with respect to a vertical axis along \$\partial\Omega\$. A variational formulation of (5) and (6) consists of seeking \$\varphi\$ such that it results:

$$\int_\Omega a_{\alpha\beta} \frac{\partial \varphi}{\partial x_\alpha} \frac{\partial \delta \varphi}{\partial x_\beta} d\Omega + \int_\Omega q \delta \varphi d\Omega = 0 \quad (7)$$

for each \$\delta\varphi\$ that vanishes on \$\partial\Omega\$. It is not difficult to show that the no-tension model for the masonry implies that \$\varphi\$ in addition must be concave (Giaquinta and Giusti, 1985).

3. Thrust network approach

Conforming finite element formulations of (7) are obtained on introducing \$C^1\$ approximations \$\hat{f}\$ of the shape function \$f\$ and \$C^0\$ approximations \$\hat{\varphi}\$ of the stress function \$\varphi\$. We hereafter instead consider a partially non-conforming scheme (cf. Ciarlet, 1978), which assumes \$C^0\$ approximations to both \$f\$ and \$\varphi\$, i.e. polyhedral test functions \$\hat{f}\$ and \$\hat{\varphi}\$ defined on a triangulation \$\Omega_h\$ of \$\Omega\$ (Fig. 2).

Such an approximation scheme leads to the following discrete version of (7):

$$\sum_{\text{edges}} \hat{A}_i^j \frac{\hat{\varphi}_j - \hat{\varphi}_i}{h_i^j} (\delta \hat{\varphi}_j - \delta \hat{\varphi}_i) + \sum_{\text{nodes}} Q_i \delta \hat{\varphi}_i = 0, \quad (8)$$

where \$h_i^j\$ is the length of the edge of \$\Omega_h\$ connecting nodes \$i\$ and \$j\$; \$\hat{\varphi}_1, \dots, \hat{\varphi}_N\$ are the nodal values of \$\hat{\varphi}\$; \$\hat{A}_i^j\$ is the jump of the derivative \$\partial \hat{f} / \partial n\$ along the normal to the edge \$i-j\$; \$Q_i\$ is the resultant vertical force in correspondence with node \$i\$.

It is not difficult to show that (8) corresponds to the system of linear algebraic equations:

$$R_i = \sum_j \hat{P}_i^j \frac{\hat{f}_j - \hat{f}_i}{h_i^j} - Q_i = \sum_{j,k} U_{ijk} \hat{\varphi}_j \hat{f}_k - Q_i = 0, \quad i = 1, \dots, N, \quad (9)$$

In (9), \$\hat{P}_i^j\$ is the jump of the normal derivative \$\partial \hat{\varphi} / \partial n\$ across the edge \$i-j\$ of \$\Omega_h\$; \$U_{ijk}\$ are coefficients depending only on the geometry of the mesh; the summations are extended to all the nodes connected to the node \$i\$; and \$N\$ is the total number of nodes forming \$\Omega_h\$. One can regard the quantities \$\hat{P}_i^j\$ as the axial forces carried by the bars of a planar truss structure having the same geometry of the skeleton of \$\Omega_h\$. Analogously, one can look at the quantities \$\hat{P}_i^j (\hat{f}_j - \hat{f}_i) / h_i^j\$ as the axial forces carried by the spatial truss \$S_h\$, which is obtained from \$\Omega_h\$ through the mapping \$x_3 = \hat{f}(x_1, x_2)\$. Eq. (9) furnishes the nodal equilibrium equations of \$S_h\$, associating a unique polyhedral stress function \$\hat{\varphi}\$ to a given polyhedral shape function \$\hat{f}\$, and vice-versa. A concave polyhedral stress function \$\hat{\varphi}\$ gives rise to all compressive forces in the bars of \$S_h\$ and \$\Omega_h\$. It is worth noting that the modeling of a continuous membrane through a pin-jointed bar network actually corresponds to a non-conforming (or external) variational approximation of the membrane equilibrium problem.

4. Constrained TNA

Let us assume that the vertical load \$q\$ and the boundary values of \$\hat{f}\$ and \$\hat{\varphi}\$ on \$\partial\Omega_h\$ are prescribed. The search for the corresponding thrust surface consists of seeking a couple \$(\hat{f}, \hat{\varphi})\$ such that the discrete equilibrium equation (9) is satisfied, under geometry constraints of the form

$$\hat{f}_i^{lb} \leq \hat{f}_i \leq \hat{f}_i^{ub} \quad (i = 1, \dots, N), \quad (10)$$

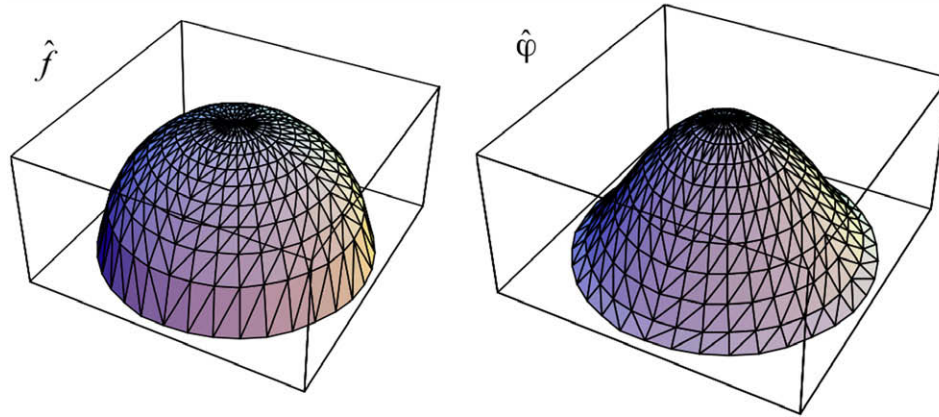


Fig. 2. Polyhedral approximations to f (left) and φ (right).

and the concavity constraint on $\hat{\varphi}$. Limitations (10) require that the thrust surface is contained in a given 3D domain D , coinciding either with the region comprised between the extrados and the intrados of an existing vault, or with a suitable design space. A constrained thrust network approach (CTNA) can be formulated as follows, assuming that an initial guess \hat{f}^0 of \hat{f} is available:

- (1) compute $\hat{\varphi}^0$ from the linear system $(U_{ijk}\hat{f}_k^0)\hat{\varphi}_j^0 = Q_i$;
- (2) compute the “concave-hull” $\hat{\varphi}'$ of $\hat{\varphi}^0$;
- (3) compute a new shape function \hat{f}' from the linear system $(U_{ijk}\hat{\varphi}_j)\hat{f}'_k = Q_i$;
- (4) if \hat{f}' satisfies the geometry constraints (10) stop with $\hat{f} = \hat{f}'$ and $\hat{\varphi} = \hat{\varphi}'$; otherwise correct \hat{f}' so as to verify (10), set $\hat{f}^0 = \hat{f}'$ and go back to 1.

Overall, the CTNA admits the quantities $Q_i, \hat{f}_i^{lb}, \hat{f}_i^{ub}$ ($i = 1, \dots, N$), and the nodal values of \hat{f} and $\hat{\varphi}$ on $\partial\Omega_h$ as input. It produces the quantities $\hat{f}_i, \hat{\varphi}_i$ at the inner nodes of Ω_h as output, according to the elastic no-tension model of masonry (cf. Giaquinta and Giusti, 1985; Del Piero, 1989). It is worth noting that the concave-hull construction of step (2) provides topological adaption of the current force network, while step (3) performs geometrical adaption (see the results of the next section). The CTNA allows one to obtain a statically admissible, purely compressive thrust network. This ensures the stability of the structure under consideration, according to the master ‘safe’ theorem of no-tension materials (Heyman, 1966, 1995; Del Piero, 1998), if the geometrical constraints (10) can be satisfied. The no-tension model assumes that fracture damage can occur in regions where the material is subject either to zero stress, or uniaxial compressive stress. In the latter case, frac-

tures are expected to run along the compressive principal stress directions. Once the solution $(\hat{f}, \hat{\varphi})$ of the CTNA is known, one can predict the portions of S_h and Ω_h exposed to fracture, as it will be shown in the next section. The continuum limit φ of the polyhedral stress function $\hat{\varphi}$ will exhibit either a flat (zero stress) or a single-curvature (uniaxial stress) profile in correspondence with such regions. Cracks will run at the extrados if the thrust surface lies towards the intrados, and vice-versa.

5. Numerical examples

In order to show how the CTNA operationally works and its capability in predicting the state of stress and the crack pattern of real masonry structures, we applied such a procedure to some benchmark examples, examining the equilibrium problems of a hemispherical dome, a groin vault, and a cloister vault.

Fig. 2-left shows the examined hemispherical dome (co-latitude opening equal to 0.9π), while Fig. 2-right illustrates the stress function $\hat{\varphi}$ obtained by letting \hat{f} coincide with the middle-surface, and applying a uniform vertical load per unit area of the platform. The above stress function assumes a convex shape towards the basis of the structure, which is associated with not-admissible circumferential tensile stresses. The concave-hull construction is able to transform the initial guess of Fig. 2-right into the concave profile shown in Fig. 3-left, which corresponds to the no-tension thrust network depicted in Fig. 3-right. The latter predicts biaxial compression towards the crown of the dome, and uniaxial meridian compression towards the basis. We are hence lead to predict a meridional crack pattern near the basis of the structure (“orange-

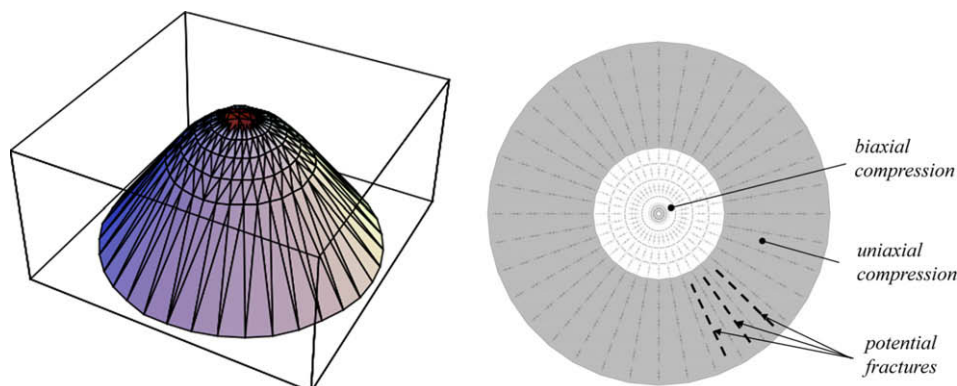


Fig. 3. Stress function (left), thrust network and potential crack pattern (right) of a hemispherical dome under uniform vertical loading.

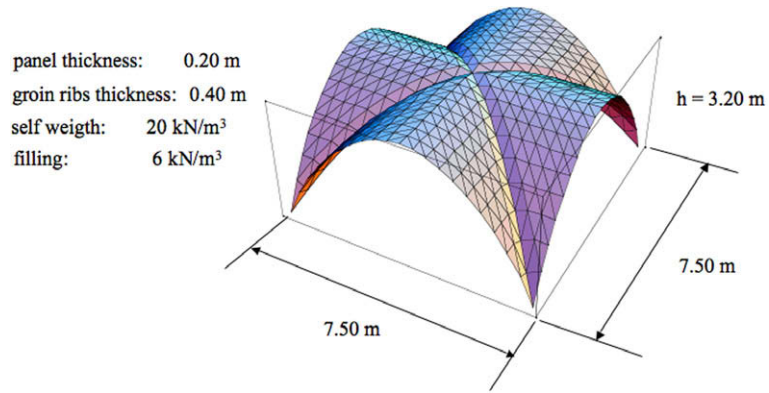


Fig. 4. Geometry and loading data for a groin vault.

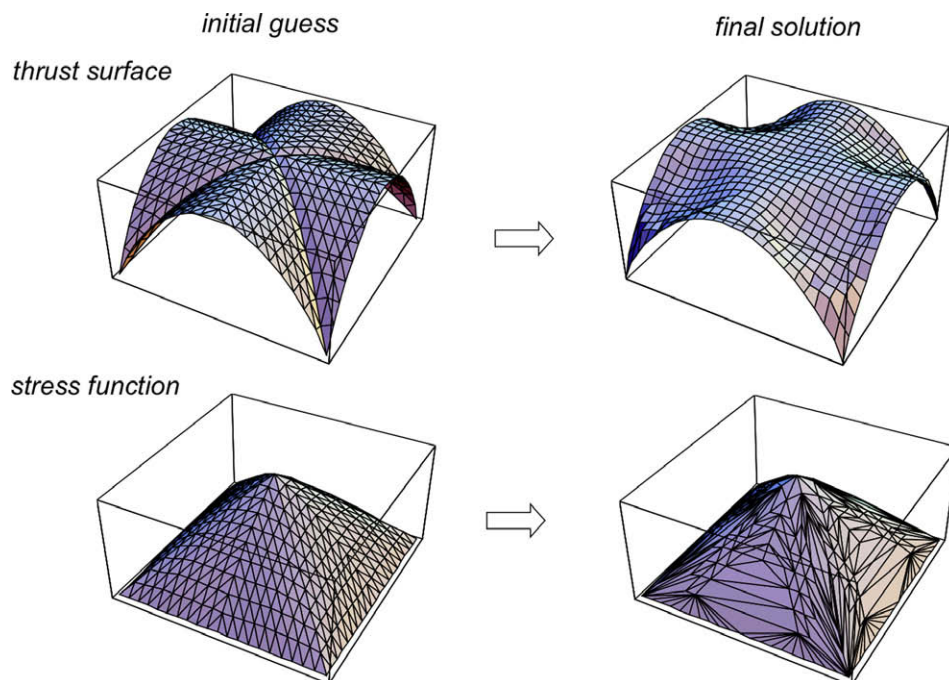


Fig. 5. Thrust surface and stress function of an unreinforced groin vault under vertical loading.

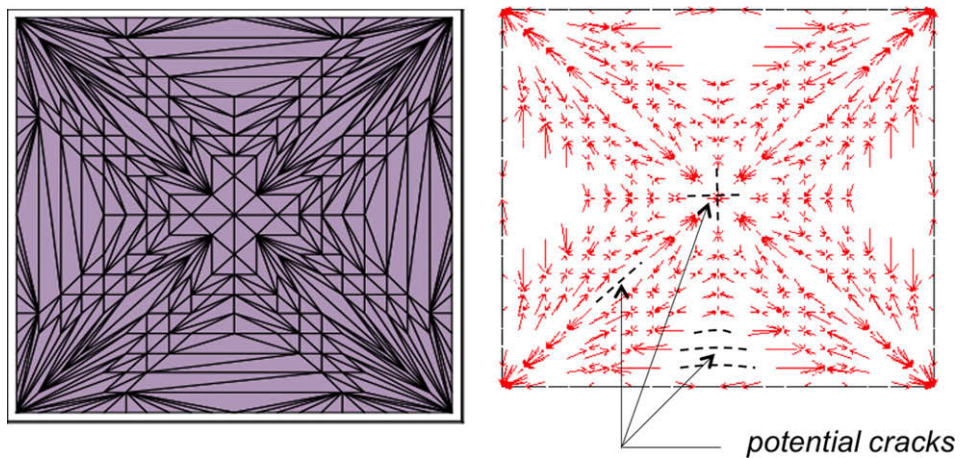


Fig. 6. Final meshing (left) and force network (right) of a groin vault under vertical loading.

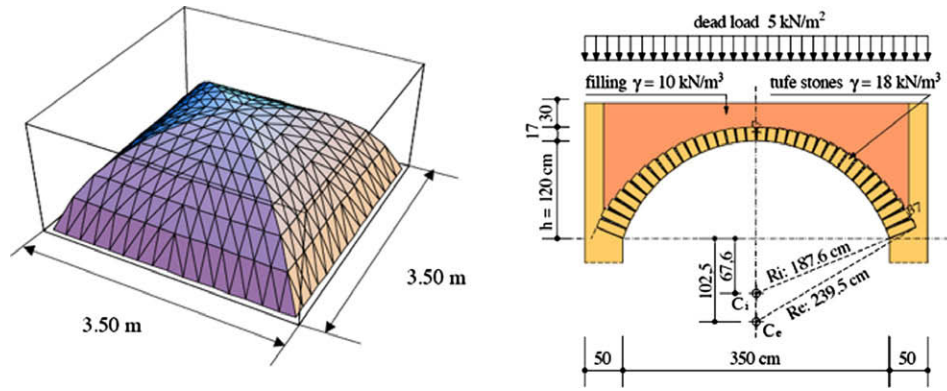


Fig. 7. Geometry and loading data for a cloister vault.

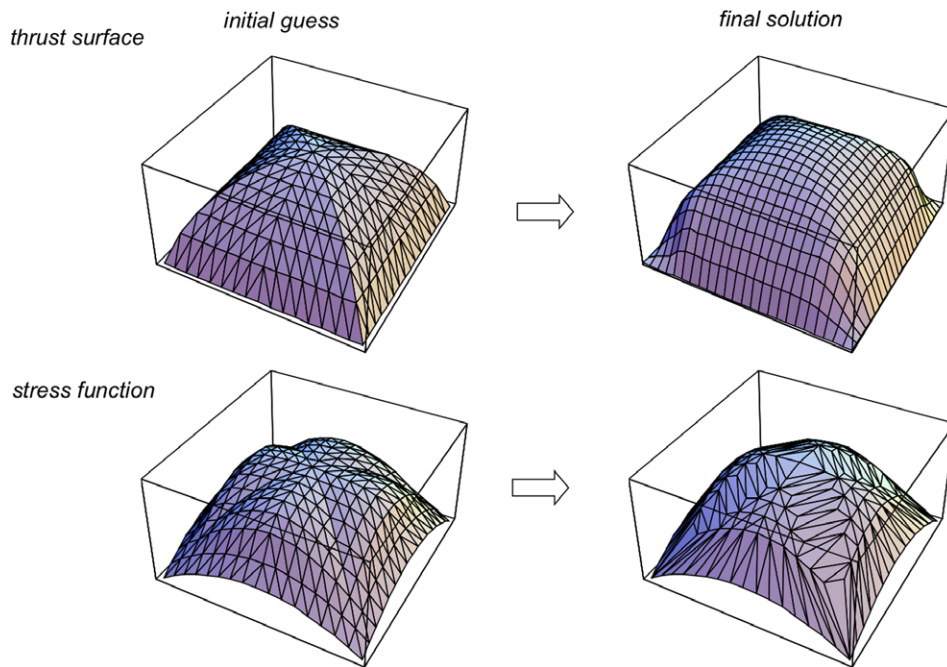


Fig. 8. Thrust surface and stress function of an unreinforced cloister vault under vertical loading.

slice” cracking mode), accordingly to what is observed in many real masonry domes of similar shape (cf. e.g. Heyman, 1995).

The second example deals with a groin vault with base dimensions $7.5 \text{ m} \times 7.5 \text{ m}$, parabolic web panels of thickness 20 cm, diagonal ribs of thickness 40 cm, and maximum rise equal to 3.2 m. The vault has self-weight of 20 kN/m^3 , and bears a material with weight of 6 kN/m^3 filling the space in between the extrados and the horizontal plane through the vertex (Fig. 4). We assumed $\hat{\varphi} = 0$ and let \hat{f} coincide with the middle-surface on $\partial\Omega_h$. The quantities \hat{f} , $\hat{\varphi}$, \hat{P}_i and the potential crack pattern obtained for the present example are illustrated in Figs. 5 and 6. One observes from Figs. 5 and 6 that cracks may run parallel to the wall ribs at the extrados (“Sabouret” cracks), along the groin ribs, and near the crown at the intrados of the examined vault, which is in good agreement with the cracking “pathology” frequently observed in real quadripartite vaults (cf. Heyman, 1995; Como, 2010). As a matter of fact, the final profile of the stress function shown in Fig. 5 bottom-right, and the associated thrust network depicted in Fig. 6-right, indicate that the no-tension state of stress is uniaxial in such regions. The topology of the final thrust network is illustrated in Fig. 6-left.

As a final example, we examine the cloister vault shown in Fig. 7, which has a $3.5 \text{ m} \times 3.5 \text{ m}$ wide platform, and maximum rise of 1.2 m. The vault is made of tufe bricks with unit weight of 18 kN/

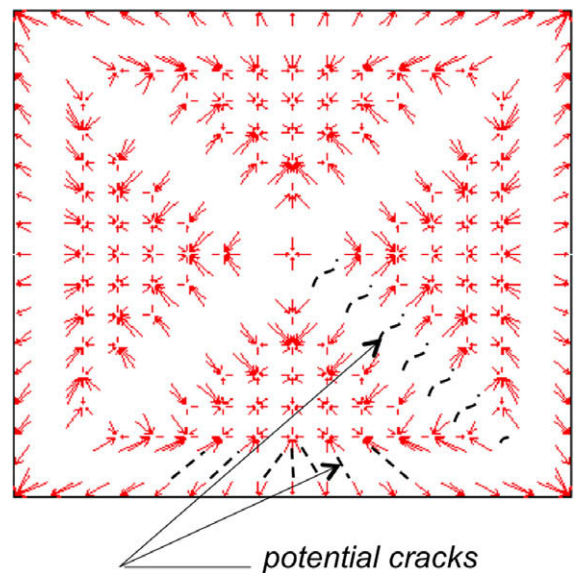


Fig. 9. Potential crack pattern of a cloister vault under vertical loading.

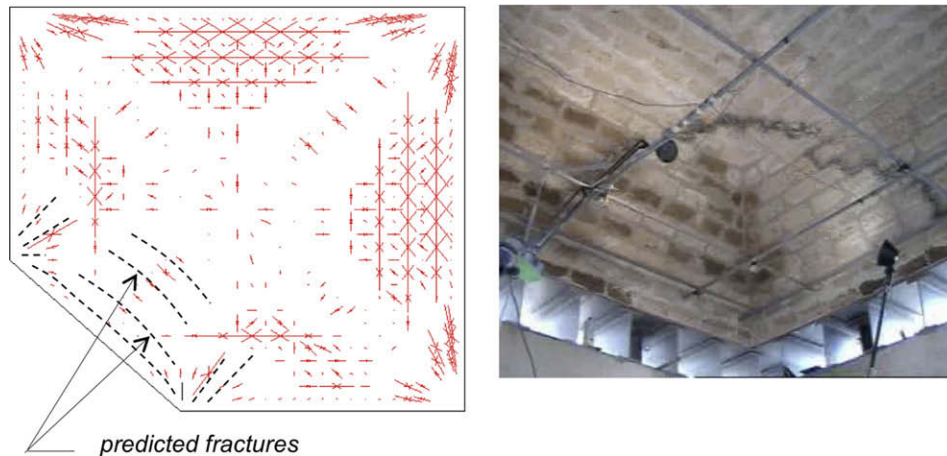


Fig. 10. Comparison between predicted (left) and experimentally observed (right) fracture damage of a cloister vault under the combined action of vertical loads and vertical movements of corner supports.

m^3 , and thickness varying from 37 cm to 17 cm. It carries the self-weight, a filling of 10 kN/m^3 , and a dead load of 18 kN/m^2 per unit area of the platform (cf. Fig. 7).

The thrust surface \hat{f} , the stress function $\hat{\phi}$, and the forces \hat{P}_i^j obtained for such a vault through the CNTA are illustrated in Figs. 8 and 9. In this case, we assumed $\hat{\phi} = \hat{\mu}$ on $\partial\Omega_h$, with $\hat{\mu}$ computed from a finite element analysis of the vault under simply supported boundary conditions (Formato, 2007). The results presented in Figs. 8 and 9 underline that the crack pattern of the vault under examination may include diagonal fractures along the web joints and radial fractures along the walls at the extrados, in conjunction with crown cracks at the intrados (we refer e.g. to Tomasoni (2008) for typical cracking mechanisms of cloister vaults). We analyzed the cloister vault also under the combined action of vertical loads and upward/downward movements of the base supports, in correspondence with a corner of the supporting perimeter. For this case, we compared the CNTA predictions with an experimental study carried out on a real scale sample of the structure (Formato, 2007). Fig. 10-left shows the numerically computed thrust network and the associated crack pattern, while Fig. 10-right illustrates the experimentally detected cracking mechanism of the vault sample, after few cycles of lifting and release of the corner supports. One notices a rather good matching between the CNTA predictions and the experimentally observed damage.

6. Concluding remarks

The CNTA presented in this work allows for the prediction of the thrust surface and the crack pattern of unreinforced masonry vaults. Some numerical results have shown the potential of such an approach in predicting the equilibrium configuration and the crack pattern of real vaulted structures. It has been shown that the modeling of a membrane as a thrust network has a variational foundation, and that the concave-hull of the membrane stress function provides statically admissible force networks for no-tension materials, through topological and geometrical adaption of an initial candidate solution.

The no-tension constraint can be suitably relaxed and piecewise enforced over selected portions of a given structure, analyzing substructures, mixed structures, pre-defined arrangements of masonry bonds, and reinforced masonry.

It is interesting noting that the no-tension model is symmetrical of the so-called tension field model of wrinkling membranes (Mansfield, 1968; Steigmann, 1990; Wong and Pellegrino, 2006). On replacing the concavity constraint of the stress potential with

a specular convexity constraint (convex-hull technique, cf. Avis and Fukuda, 1992), one can easily generalize the CNTA presented in this work to membranes carrying only tensile stresses.

References

- Andreu, A., Gil, L., Roca, P., 2007. Computational analysis of masonry structures with a funicular model. *J. Eng. Mech. – ASCE* 133 (4), 473–480.
- Avis, D., Fukuda, K., 1992. A pivoting algorithm for convex hulls and vertex enumeration of arrangements and polyhedra. *Discrete Comput. Geomet.* 8, 295–313.
- Block, P., 2009. Thrust network analysis – exploring three-dimensional equilibrium. Ph.D. Dissertation, Massachusetts Institute of Technology, USA.
- Block, P., Ochsendorf, J., 2005. Interactive thrust line analysis for masonry structures. In: Mochi, G. (Ed.), *International Seminar on Theory and Practice of Construction: Knowledge, Means, and Models*, Ravenna, Italy, pp. 13–24.
- Block, P., Ochsendorf, J., 2007. Thrust network analysis: a new methodology for three-dimensional equilibrium. *IASS J.* 48 (3), 167–173.
- Boothby, T.E., 2001. Analysis of masonry arches and vaults. *Prog. Struct. Eng. Mater.* 3, 246–256.
- Ciarlet, P.G., 1978. *The Finite Element Method for Elliptic Problems*. North-Holland, Amsterdam.
- Como, M., 2010. *Statica delle costruzioni in muratura*. Aracne Editrice, Roma.
- Del Piero, G., 1989. Constitutive equations and compatibility of the external loads for linear elastic masonry-like materials. *Meccanica* 24, 150–162.
- Del Piero, G., 1998. Limit analysis and no-tension materials. *Int. J. Plast.* 14, 259–271.
- Di Pasquale, S., 1975. *Scienza delle costruzioni. Introduzione alla progettazione strutturale*. Tamburini, Milano.
- Formato, F., 2007. A theoretical and experimental study on the statics of masonry vaults. Ph.D. Dissertation, University of Salerno, Italy.
- Fraternali, F., 2001. Complementary energy variational approach for plane elastic problems with singularities. *Theor. Appl. Fract. Mech.* 35, 129–135.
- Fraternali, F., Angelillo, M., Fortunato, A., 2002a. A lumped stress method for plane elastic problems and the discrete–continuum approximation. *Int. J. Solids Struct.* 39, 6211–6240.
- Fraternali, F., Angelillo, M., Rocchetta, G., 2002b. On the stress skeleton of masonry vaults and domes, PACAM VII, January 2–5, 2002, Temuco, Chile, pp. 369–372.
- Giaquinta, M., Giusti, G., 1985. Researches on the equilibrium of masonry structures. *Arch. Ration. Mech. Anal.* 88, 359–392.
- Heyman, J., 1966. The stone skeleton. *Int. J. Solids Struct.* 2, 249–279.
- Heyman, J., 1977. *Equilibrium of Shell Structures*. Oxford Engineering Science Series. Clarendon Press, Oxford.
- Heyman, J., 1995. *The Stone Skeleton*. Cambridge University Press, Cambridge.
- Huerta, S., 2001. Mechanics of masonry vaults: the equilibrium approach. In: Lourenço, P.B., Roca, P. (Eds.), *Proceedings of Historical Constructions*, Guimarães, pp. 47–69.
- Kilian, A., 2007. Steering of form. *IASS J.* 48 (4), 17–21.
- Kilian, A., Ochsendorf, J., 2005. Particle-spring systems for structural form finding. *IASS J.* 46 (2), 77–85.
- Lucchesi, M., Padovani, C., Pasquinelli, G., Zani, N., 2008. *Masonry Constructions: Mechanical Models and Numerical Applications*. Lecture Notes in Applied and Computational Mechanics, vol. 39. Springer-Verlag, Berlin, Heidelberg.
- Mansfield, E.H., 1968. Tension field theory. In: Hetenyi, M., Vincenti, W.G. (Eds.), *Proceedings of the 12th International Congress on Applied Mechanics*, pp. 305–320.
- Ochsendorf, J., Block, P., 2009. Designing unreinforced masonry. In: Allen, E., Zalewski, W. (Eds.), *Form and Forces: Designing Efficient, Expressive Structures*. John Wiley Sons, New York (Chapter 8).

- O'Dwyer, D., 1999. Funicular analysis of masonry vaults. *Int. J. Solids Struct.* 73, 187–197.
- Poleni, G., 1991. *Memorie storiche della gran cupola del Tempio Vaticano*. Edizioni Kappa, Rome, Italy (Anastatic reprint of the original edition of 1748).
- Steigmann, D.J., 1990. Tension-field theory. *Proc. Roy. Soc. Lond., Ser. A, Math. Phys. Sci.* 429 (1876), 141–173.
- Tomasoni, E., 2008. *Le volte in muratura negli edifici storici. Tecniche costruttive e comportamento strutturale*. Aracne Editrice, Roma, Italy.
- Tomlow, J., Graefe, R., Otto, F., Szeemann, H. 1989. *Das Modell/The Model/El Modelo*. Number 34 in *Mitteilungen des Instituts für Leichte Flächtragwerke (IL)*. Universität Stuttgart, Stuttgart.
- Ungewitter, G., 1890. *Lehrbuch der gotischen Konstruktionen*. Weigel Nachfolger, Leipzig.
- Wittmann, W., 1879. Zur Theorie der Gewölbe. *Z. Bauwesen* 26, 61–74.
- Wong, Y.W., Pellegrino, S., 2006. Wrinkled membranes. Part I: experiments; part II: analytical models; part III: numerical simulations. *J. Mech. Mater. Struct.* 1, 1–93.